

Electronic Supplementary Information

Defective crystalline molybdenum phosphides as bifunctional catalysts for hydrogen evolution and hydrazine oxidation reactions in water splitting

Yan Gao ^{a, §}, Qiang Wang ^{b, §}, Ting He ^d, Jun-Ye Zhang ^d, Hao Sun ^a, Bin Zhao ^a, Bao Yu Xia ^d, Ya Yan ^{a, *}, Yuan Chen ^{c, *}

^a School of Materials Science & Engineering, University of Shanghai for Science and Technology, 516 Jungong Road, Shanghai 200093, R China

^b Department of Applied Chemistry, School of Chemistry and Molecular Engineering, Nanjing Tech University, Nanjing 211880, P. R. China

^c School of Chemical and Biomolecular Engineering, The University of Sydney, Sydney, New South Wales 2006, Australia

^d School of Chemistry and Chemical Engineering, Wuhan National Laboratory for Optoelectronics, Huazhong University of Science and Technology (HUST), 1037 Luoyu Road, Wuhan 430074, PR China

§ These authors contributed equally.

*Corresponding author. E-mail: yanya@usst.edu.cn (Y. Yan), yuan.chen@sydney.edu.au (Y. Chen)

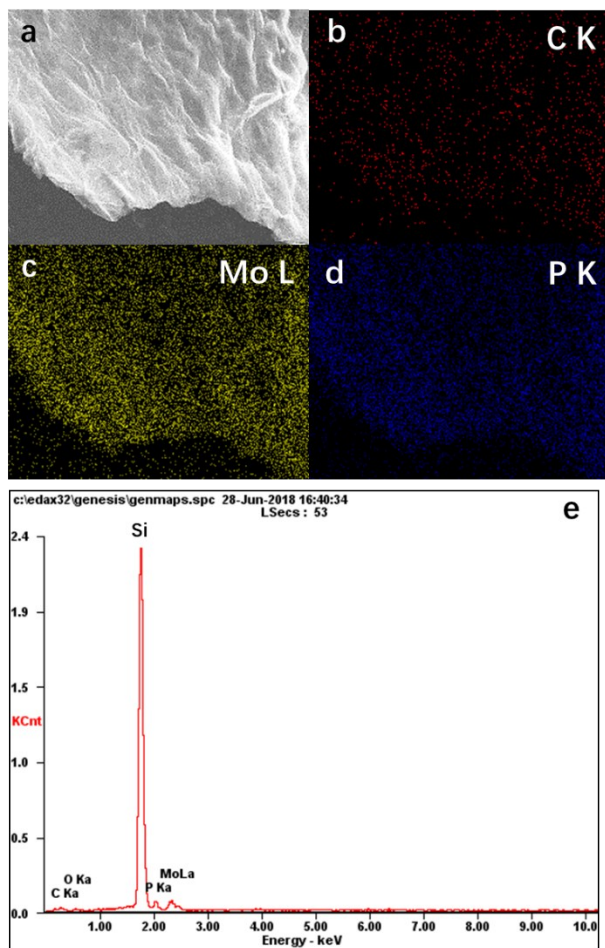


Fig. S1. An SEM image (a) and the corresponding EDS maps (b-d) and an EDS spectrum (e) of D-MoP/rGO. The Si peak in (e) comes from the Si wafer support.

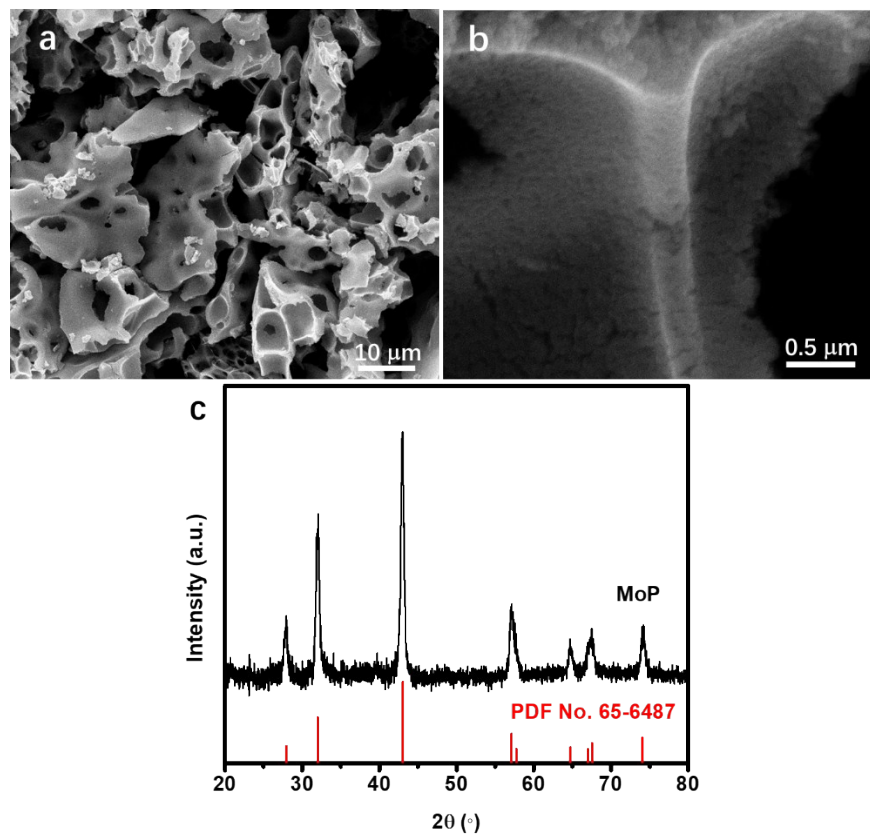


Fig. S2. (a,b) SEM images and (c) an XRD pattern of bulk MoP.

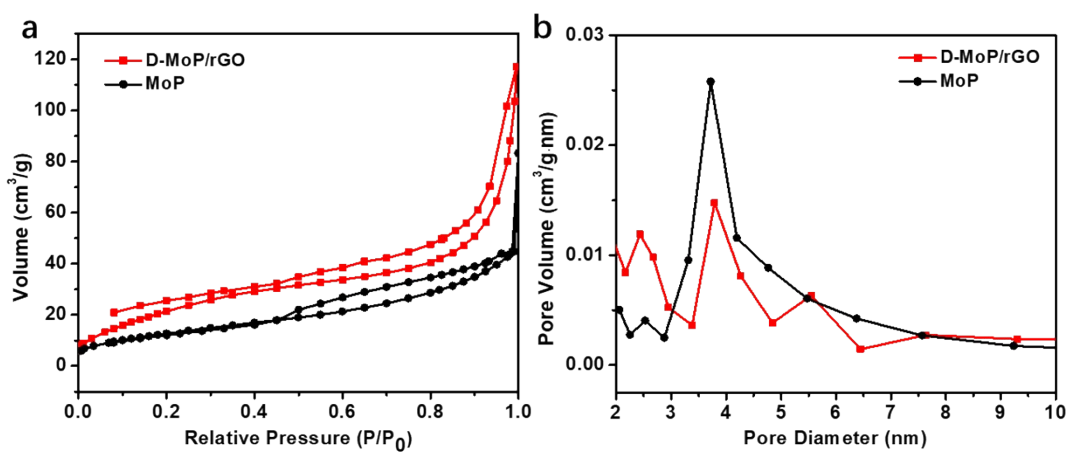


Fig. S3. (a) N_2 adsorption-desorption isotherms and (b) the pore size distribution of D-MoP/rGO in comparison with a bulk MoP sample.

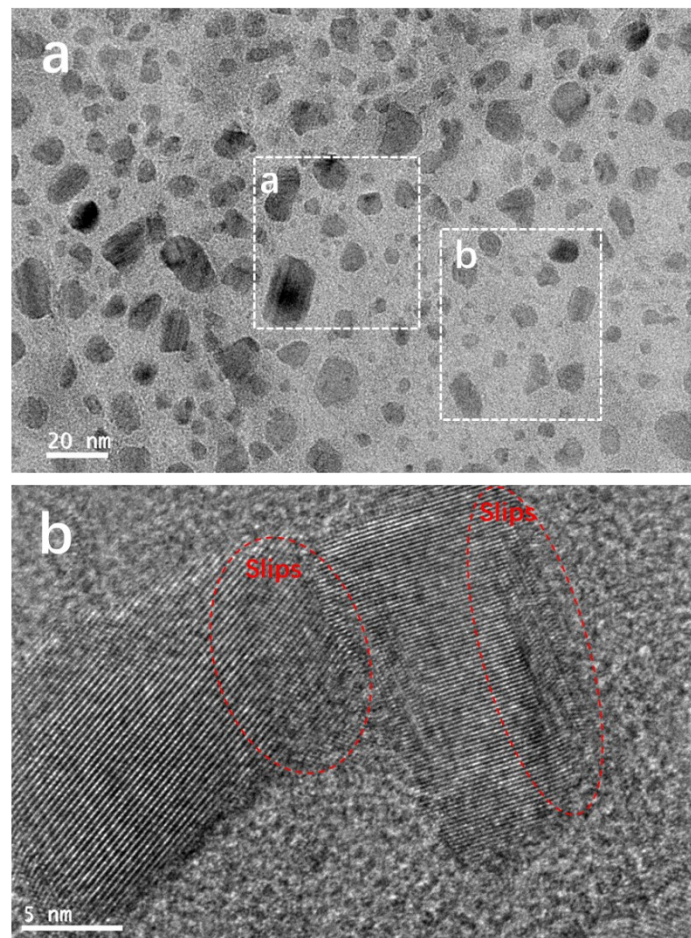


Fig. S4. The TEM images of D-MoP/rGO. (a) Figure 2a and 2b are extracted from the selected area (white squares) in this image. b) The HRTEM image of D-MoP/rGO show slips in the crystal structure of MoP.

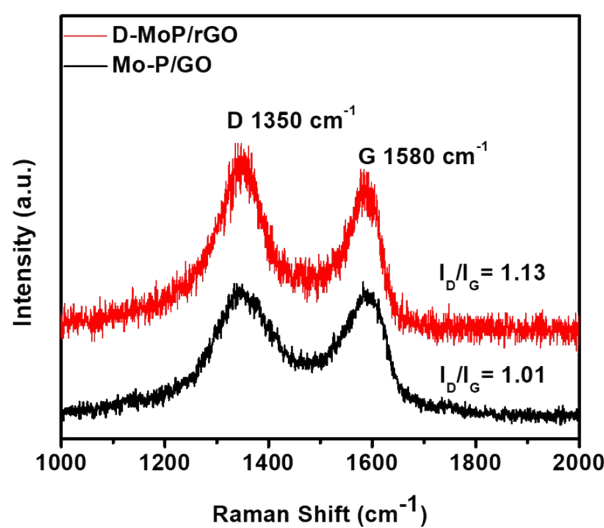


Fig. S5. Raman spectra of D-MoP/rGO and the GO supported precursors (donated as Mo-P/GO).

The Raman spectrum of D-MoP/rGO exhibits typical D and G bands of carbon materials at 1370 and 1594 cm^{-1} , respectively. The I_D/I_G ratio of D-MoP/rGO at 1.13 is much higher than that of Mo-P/GO at 1.01 . This demonstrates the present of the defects on the rGO after thermal annealing along with optimized conductively of the hybrid.

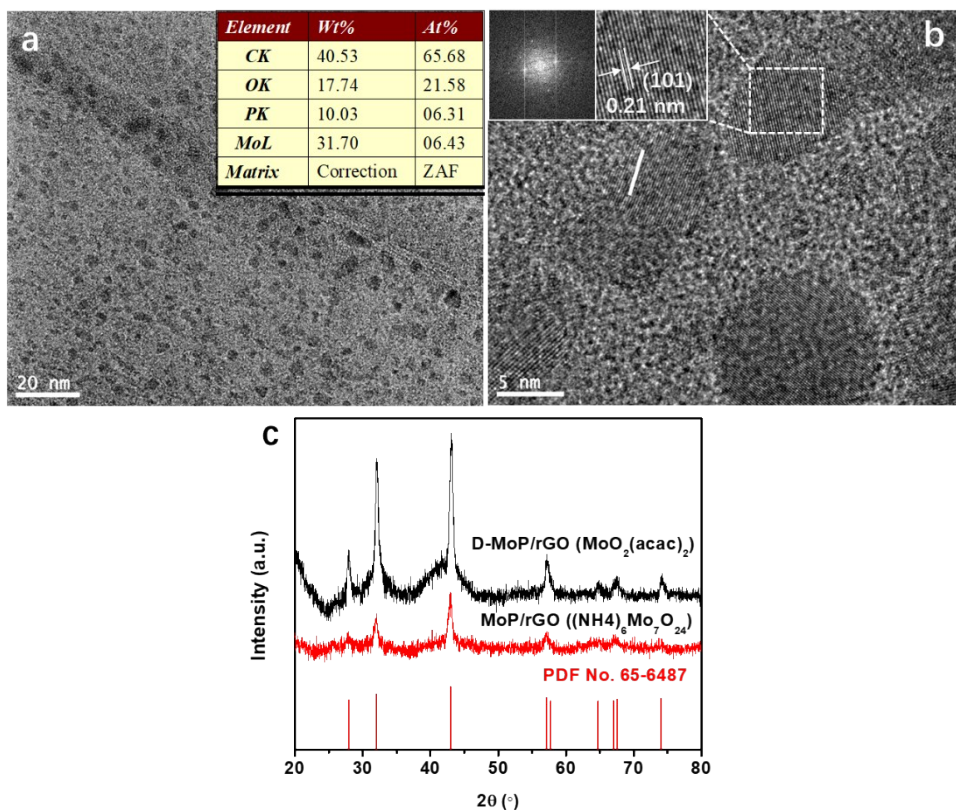


Fig. S7. Characterization of MoP/rGO synthesized by using $(\text{NH}_4)_6\text{Mo}_7\text{O}_{24}$ as the Mo precursor. (a) TEM and (b) HRTEM images of MoP/rGO. The inset of (a) is the EDX elemental distribution. (c) XRD patterns. (d) *iR*-corrected LSV polarization curves of MoP/rGO, D-MoP/rGO, and Pt/C in 1.0 M KOH.

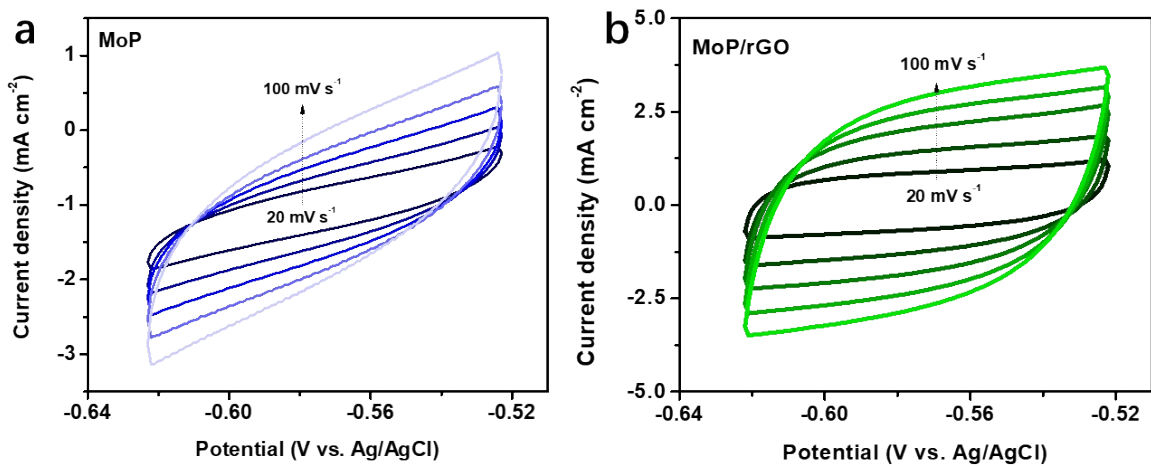


Fig. S7. CVs of bulk MoP and MoP/rGO in a non-faradaic capacitance current range at the scan rates of 20, 40, 60, 80 and 100 mV s^{-1} .

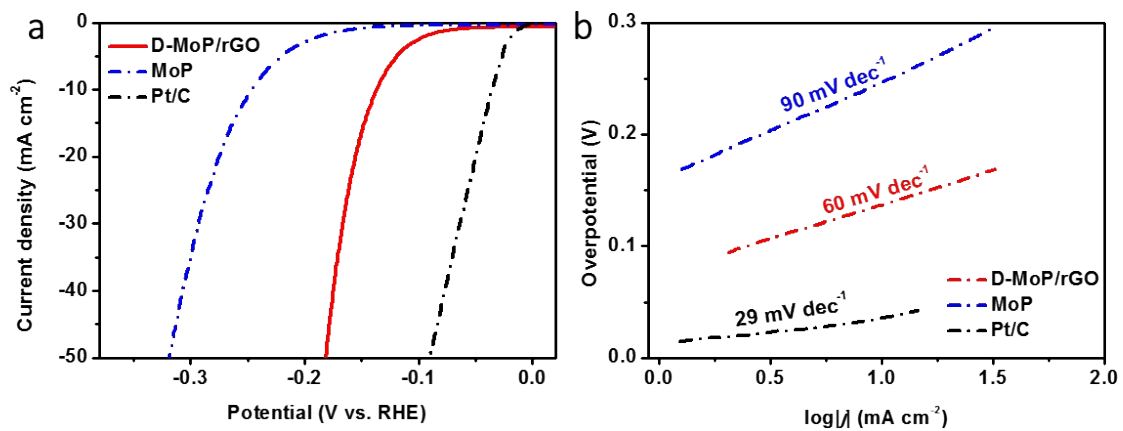


Fig. S8. (a) HER LSV polarization curves of D-MoP/rGO, MoP, and Pt/C in 0.5 M H_2SO_4 and (b) the corresponding Tafel plots.

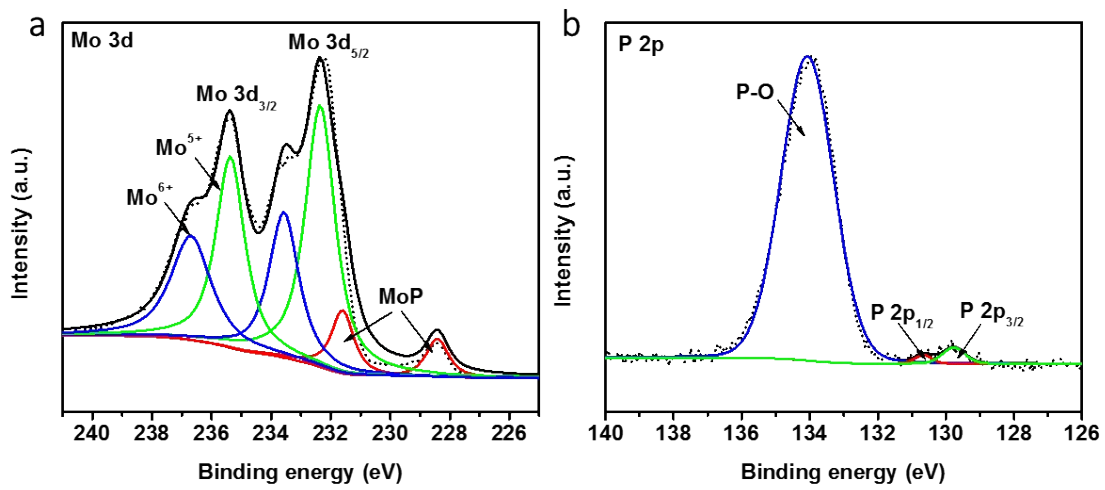


Fig. S9. XPS spectra of D-MoP/rGO after the HER test. (a) Mo 3d and (b) P 2p spectra.

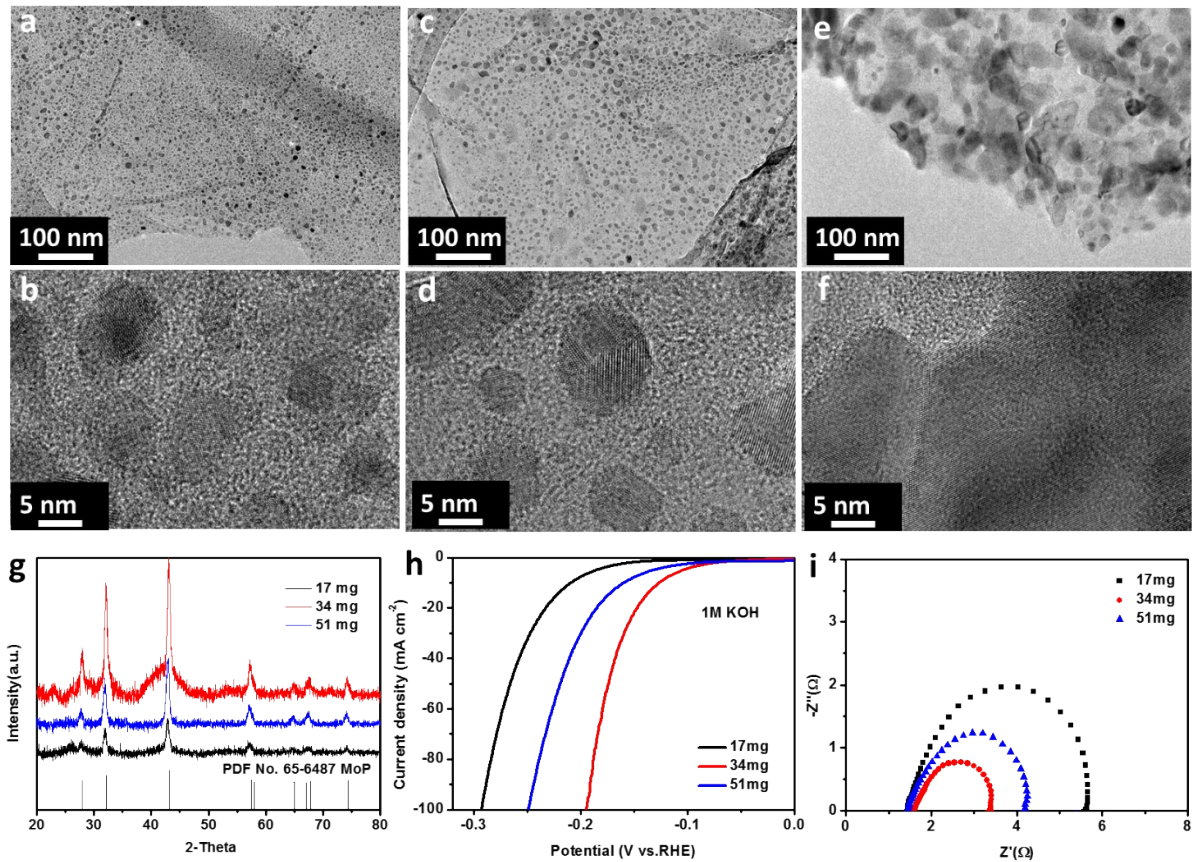


Fig. S10. TEM images of crystalline MoP/rGO synthesized using different amount of MoO₂(acac)₂, (a,b) 17 mg, (c,d) 34 mg, (e,f) 51 mg. (g) XRD patterns of these samples. (h) HER LSV polarization curves of these samples in 1.0 M KOH and (i) their corresponding Nyquist plots.

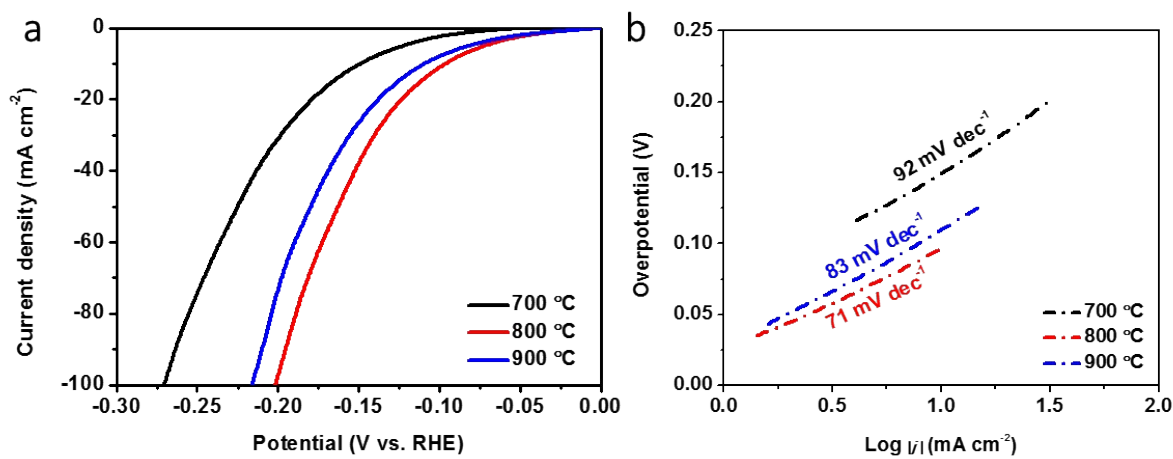


Fig. S11. HER LSV polarization curves of D-MoP/rGO synthesized at different annealing temperatures (electrolyte:1.0 M KOH)

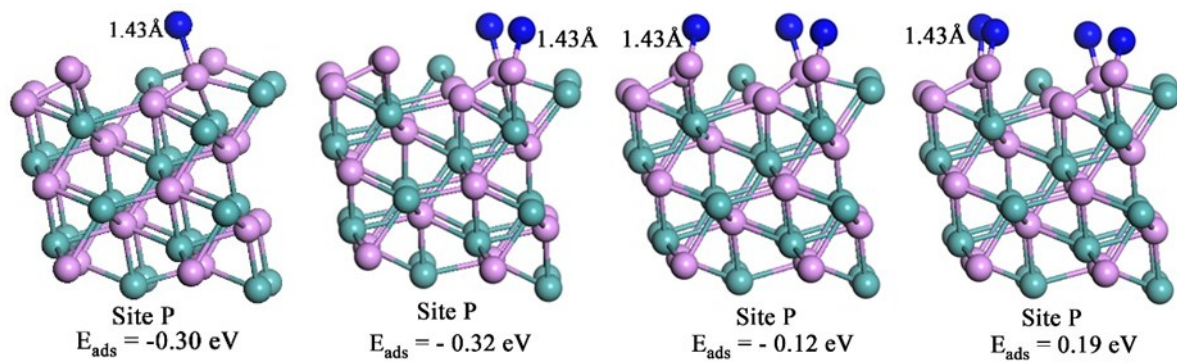


Fig. S12. Adsorption models of 1H, 2H, 3H, 4H atoms on MoP (111)-Mo surfaces.

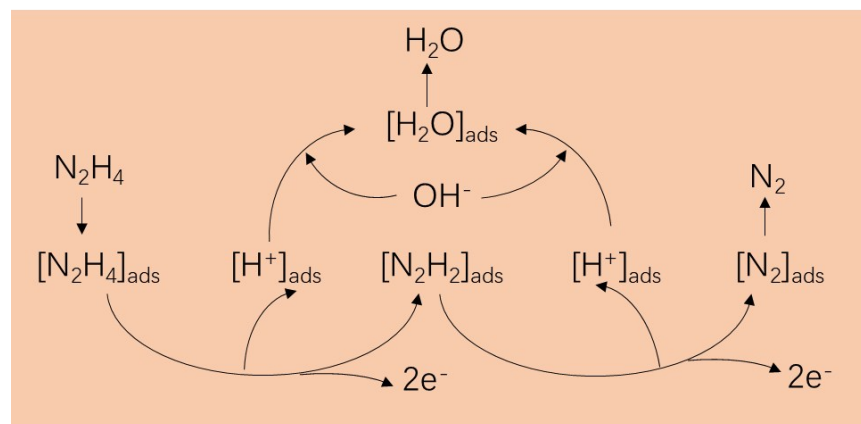


Fig. S13. Schematic illustration of the proposed reaction steps for hydrazine oxidation on D-MoP/rGO.

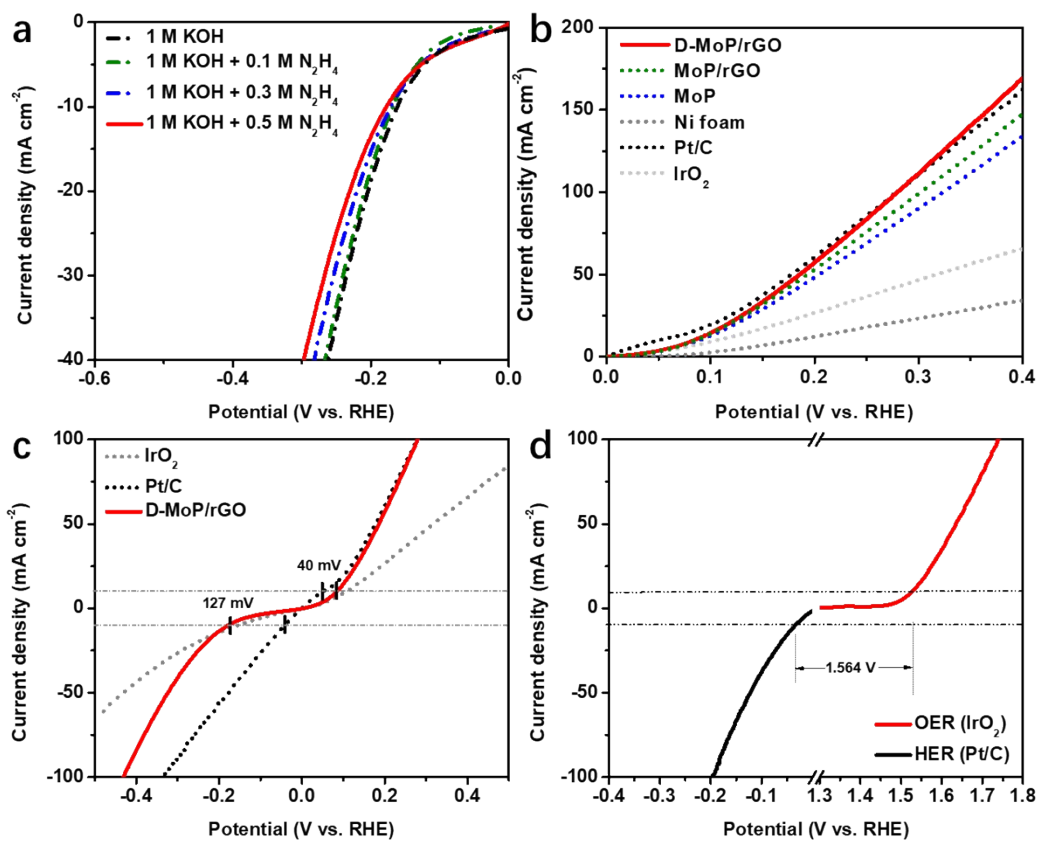


Figure S14. (a) HER LSV polarization curves of D-MoP/rGO in 1.0 M KOH containing different amount of hydrazine. (b) LSV polarization curves of various catalysts for the HER/HzOR couple in 1.0 M KOH containing 0.5 M N_2H_4 . (c) LSV polarization curves of D-MoP/rGO, Pt/C and IrO_2 for the HER/HzOR couple in 1.0 M KOH containing 0.5 M N_2H_4 . (d) LSV polarization curves of Pt/C (HER) and IrO_2 (OER) in 1.0 M KOH.

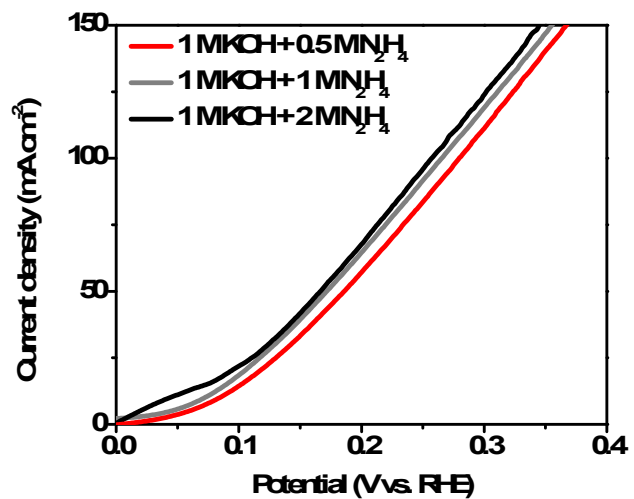


Fig. S15. LSV polarization curves of D-MoP/rGO for hydrazine oxidation in 1.0 M KOH containing hydrazine at different concentrations.

Table S1. HER activities of Mo- and P- based electrocatalysts under alkaline (1.0M KOH) media.

Catalysts	Electrolyte	η_{onset} (mV)	Tafel slope (mV dec ⁻¹)	j_{geo} (mA cm ⁻²)	Loading (mg cm ⁻²)	Reference
D-MoP/rGO	1.0 M KOH	38	71	10 @$\eta=$ 122 mV 30 @$\eta=$ 158 mV	1.5	This work
MoP/NC	1.0 M KOH	-	50	10 @ $\eta=$ 170 mV	~0.56	<i>Appl. Catal., B.</i> 2019 , 245, 656
MoP/CNTs-700	1.0 M KOH	34	73	10 @ $\eta=$ 86 mV	0.5	<i>Adv. Funct. Mater.</i> 2018 , 28, 1706523
MoP-RGO	1.0 M KOH	-	62	10 @ $\eta=$ 150 mV	0.42	<i>Electrochim. Acta</i> , 2017 , 232, 254
MoP	1.0 M KOH	50	-	30 @ $\eta=$ 180 mV	0.86	<i>Energy Environ. Sci.</i> 2014 , 7, 2624
MoCx nano-octahedrons	1.0 M KOH	80	59	10 @ $\eta=$ 151 mV	0.8	<i>Nat. Commun.</i> 2015 , 6,6512
Ni-MoS ₂	1.0 M KOH	45	60	10 @ $\eta=$ 98 mV	0.89	<i>Energy Environ. Sci.</i> 2016 , 9, 2789
MoO ₂	1.0 M KOH	0	41	10 @ $\eta=$ 10 mV	2.9	<i>Adv. Mater.</i> , 2016, 28, 3785-3790
FeP NAs/CC	1.0 M KOH	86	146	10 @ $\eta=$ 218 mV	1.5	<i>ACS Catal.</i> 2014 , 4, 4065
Ni ₅ P ₄ (pellet)	1.0 M NaOH	-	98	10 @ $\eta=$ 49 mV	50 mg in 6 mm pellet	<i>Energy Environ. Sci.</i> 2015 , 8, 1027
Ni ₂ P(pellet)	1.0 M NaOH	-	118	10 @ $\eta=$ 69 mV		
Porous Co phosphide/Co phosphate thin film	1.0 M KOH	-	-	30 @ $\eta=$ 430 mV	0.1	<i>Adv. Mater.</i> 2015 , 27, 3175
Co-P film	1.0 M KOH	-	42	10 @ $\eta=$ 94 mV	Co=2.52 P=0.19	<i>Angew. Chem. Int. Ed.</i> 2015 , 54, 6251
Ni _{0.33} Co _{0.67} S ₂	1.0 M KOH	50	118	10 @ $\eta=$ 88 mV	0.3	<i>Adv. Energy Mater.</i> 2015 , 5, 1402031

Table S2. The values of ΔE_{H^*} , $\Delta E_{\text{ZPE}(\text{H}^*)}$, ΔE_{ZPE} and ΔG_{H^*} of H^* at the surface of MoP (111) and MoP (111)-Mo.

		$\Delta E_{\text{H}^*}/\text{eV}$	$\Delta E_{\text{ZPE}(\text{H}^*)}/\text{eV}$	$\Delta E_{\text{ZPE}}/\text{eV}$	$\Delta G_{\text{H}^*}/\text{eV}$
MoP (111)	1H	-0.300813	0.206958	0.069122	-0.43
	2H	-0.292545	0.413850	0.276014	-0.22
	3H	-0.097355	0.616084	0.478248	0.18
	4H	-0.068716	0.816629	0.678793	0.41
MoP (111)-Mo	1H	-0.299527	0.210584	0.072748	-0.43
	2H	-0.324443	0.420035	0.282199	-0.24
	3H	-0.120011	0.622901	0.485064	0.16
	4H	0.193886	0.792931	0.655095	0.65

Table S3. Cell voltage of different electro-catalysts for overall water splitting.

Catalysts	Electrolyte	Cell voltage (V)	Current density (mA cm^{-2})	Durability (h)	Reference
D-MoP/rGO	1.0 M KOH +0.5 M N₂H₄	0.74	100	12	<i>This work</i>
Cu ₃ P/CF	1.0 M KOH +0.5 M N ₂ H ₄	0.4	10	3	<i>Inorg. Chem. Front.</i> 2017 , 4, 420
Ni ₂ P/NF	1.0 M KOH +0.5 M N ₂ H ₄	0.45	100	10	<i>Angew. Chem. Int.Ed.</i> 2017 , 129, 860-864
CoP/TiM	1.0 M KOH +0.1 M N ₂ H ₄	0.3	40	5.5	<i>ChemElectroChem</i> 2017 , 4, 481
Tubular CoSe ₂ nanosheet	1.0 M KOH +0.5 M N ₂ H ₄	0.164	10	14	<i>Angew. Chem. Int. Ed.</i> 2018 , 57, 7649
Ni ₂ P NF/CC	1 M KOH +0.5 M urea	1.35	50	-	<i>J. Mater. Chem. A</i> 2017 , 5, 3208
Co-P/rGO	1.0 M NaOH	1.70	10	-	<i>Chem. Sci.</i> , 2016 , 7, 1690
FeP NTs	1.0 M KOH	1.69	10	14	<i>Chem. Eur. J.</i> 2015 , & 21, 1
Cu@NiFe LDH	1.0 M KOH	1.54	10	48	<i>Energy Environ. Sci.</i> 2017 , 10, 1820
NiFeOx/CFP	1.0 M KOH	1.51	10	200	<i>Nat. Commun.</i> 2015 , 6, 7261
Co ₁ Mn ₁ CH/NF	1.0 M KOH	1.68	10	-	<i>J. Am. Chem. Soc.</i> 2017 , 139, 8320